ARCTIC
VOL. 77, NO. 1 (MARCH 2024) P. 1–12
https://doi.org/10.14430/arctic79155

Tall and Low Shrub-Adapted Passerines Respond Differently to Shrub Expansion in Arctic and Subarctic Alaska

Jeremy D. Mizel[1]

(*Received 18 July 2023; accepted in revised form 13 October 2023*)

ABSTRACT. The expansion of deciduous shrubs is among the most conspicuous and widespread of the phenomena affecting tundra regions under a warming climate. While this process is expected to affect the distributions of terrestrial vertebrates, empirical assessments of responses to shrub expansion are rare, particularly for passerine birds. Here, I jointly investigate the topographic correlates of shrub expansion and differences in the density of shrub-adapted passerines between long- and recently established shrub cover at five sites in Arctic and Subarctic Alaska. I used a remotely sensed vegetation cover timeseries (1985–2020) and line transect data (2015–22) for four low and four tall shrub–adapted passerines. The line transect data were comprised of the individual encounter locations, which permitted fine-scale assessment of the effect of shrub cover age class (established pre- or post-1985) under a point process framework. Low shrub–adapted species showed weak differences in density between long- (pre-1985) and recently established (post-1985) shrub cover. In contrast, a subset of tall shrub–adapted species at two of the five study areas had lower density where the proportion of total shrub cover in the younger age class was relatively high. The contrasting responses of these two groups suggest that expanding shrub cover may have structural characteristics, such as shorter height and a more diffuse distribution, that are not preferred by tall shrub–adapted passerines. This suggests caution in assuming uniform responses to shrub expansion across species and spatial regions and indicates the potential importance of incorporating time lags into assessments of vertebrate responses to shrub expansion.

Keywords: birds; climate change; density surface models; spatial distance sampling; time lags; tundra

RÉSUMÉ. L'extension des arbustes à feuillage caduc fait partie des phénomènes les plus visibles et répandus des régions de la toundra en temps de réchauffement climatique. Bien qu'on s'attende à ce que ce processus ait un effet sur la répartition des vertébrés terrestres, les évaluations empiriques des réactions à l'extension des arbustes se font rares, surtout dans le cas des passereaux. Dans cet article, je me penche conjointement sur les corrélats topographiques de l'extension des arbustes ainsi que sur les différences en matière de densité des passereaux adaptés aux arbustes entre le couvert arbustif de longue date et le couvert arbustif récent à cinq sites de l'Arctique et de l'Alaska subarctique. Je me suis appuyé sur les séries chronologiques du couvert végétal obtenues par télédétection (1985–2020) et sur les données de transects linéaires (2015–2022) pour quatre passereaux adaptés aux petits arbustes et quatre passereaux adaptés aux grands arbustes. Les données émanant des transects linéaires comprenaient des données sur les emplacements des rencontres individuelles, ce qui a permis de faire une évaluation à petite échelle de l'effet du couvert arbustif en fonction de sa catégorie d'âge (établi avant ou après 1985) en fonction d'un cadre de processus ponctuel. Les espèces adaptées aux petits arbustes ont affiché de faibles différences de densité entre le couvert arbustif de longue date (avant 1985) et le couvert arbustif récent (après 1985). Par contraste, un sous-ensemble d'espèces adaptées aux grands arbustes recueilli à deux des cinq sites étudiés affichait une densité plus faible, là où la proportion du couvert arbustif total de la catégorie d'âge plus jeune était relativement élevée. Les réactions contrastées de ces deux groupes suggèrent que le couvert arbustif en extension pourrait posséder des caractéristiques structurales qui ne sont pas privilégiées par les passereaux adaptés aux grands arbustes, comme une moins grande hauteur et une distribution plus diffuse. Cela suggère qu'il y a lieu de faire preuve de prudence avant de présumer que les réactions au couvert arbustif en extension sont uniformes pour toutes les espèces et les régions spatiales. Cela indique également l'importance éventuelle d'intégrer les séries chronologiques aux évaluations des réactions des vertébrés vis-à-vis de l'extension des arbustes.

Mots-clés : oiseaux; changement climatique; modèles de surface de densité; échantillonnage de distance spatiale; séries chronologiques; toundra

Traduit pour la revue *Arctic* par Nicole Giguère.

Arctic Network, U.S. National Park Service, 4175 Geist Road, Fairbanks, Alaska 99709, USA; jeremy_mizel@nps.gov
© The Arctic Institute of North America

INTRODUCTION

The expansion of deciduous shrubs is among the most conspicuous and widespread of the phenomena affecting Arctic and Subarctic tundra regions under a warming climate (e.g., Sturm et al., 2001; Tape et al., 2006; Myers-Smith et al., 2011). Such changes in vegetation structure and composition are expected to affect the distribution of vertebrates (reviewed in Wheeler et al., 2018). For example, the recent range expansions of moose (*Alces alces gigas*) and snowshoe hare (*Lepus americanus*) in Arctic Alaska appear to be linked to riparian shrub expansion in the region (Tape et al., 2016a, b). However, for many species and, particularly, passerine birds, empirical assessments of responses to shrub expansion are rare.

In one such assessment, Mizel et al. (2023) found weak above-treeline responses to recent deciduous shrub (shrub) expansion (1995–2020) among shrub-adapted passerines in Denali National Park and Preserve (Denali), Alaska. While the scale of shrub expansion in above-treeline portions of their study area was relatively modest, other factors may have been involved in the weak response. For example, dwarf birch (*Betula nana*) may represent a large component of the observed shrub colonization, as evidenced by its widespread expansion in the Low Arctic (Tape et al., 2006) and near treeline, Subarctic regions (Ropars and Boudreau, 2012). Dwarf birch supports a lower biomass of arthropod prey compared to willow (*Salix*) and, consequently, may represent suboptimal habitat for shrub-adapted passerines (McDermott et al., 2021). In addition, the observed above-treeline shrub expansion may have been relatively diffuse and short statured as opposed to the tall and large thickets that appear to be the preferred habitat structure for shrub-adapted birds (Henden et al., 2013). The potential existence of variation in the floristic composition, stature, canopy volume, and spatial dispersion between long- and recently established shrub cover could have important implications for passerine distribution.

Here, I jointly investigate the topographic correlates of shrub expansion and differences in the density of shrub-adapted passerines between long- and recently established shrub cover at five sites in Alaska; three in the Arctic and two in the Subarctic (Fig. 1). I begin by using a remotely sensed vegetation cover timeseries (Macander and Nelson, 2022) to assess the topographic correlates of expanding shrub cover (deciduous shrubs <500 cm in height) between 1985 and 2020. Based on previous work, I expected shrub colonization rates to be higher in proximity to pre-existing shrub cover, at lower elevations, on mesic sites, and at intermediate snow-free dates (e.g., Sturm et al., 2005; Brodie et al., 2019; Mizel et al., 2023).

I then assess differences in the current density of shrub-adapted passerines between long-established (pre-1985) and recently established (post-1985) shrub cover using distance sampling (line transect) data collected between 2015 and 2022. These data were unique in the sense that they are comprised of individual-encounter locations rather than counts aggregated at the plot level, thereby allowing fine-scale assessment of spatial variation in density under a point process framework (Hedley and Buckland, 2004; Mizel et al., 2018). I expected that the effect of shrub-cover age class (pre- or post-1985) would vary across study areas and species due to species-specific habitat requirements and study area–specific variation in the structural characteristics of recently established shrub cover. Further, I expected low shrub–adapted species (those associated with shrub heights of 0.4–1.1 m; Kessel, 1979) would show weak effects of shrub-cover age class, while tall shrub–adapted species (those associated with shrub heights of 1.2–4.9 m; Kessel, 1979) would show reduced density in recently established shrub cover. I hypothesized that such a response might arise if shrub expansion primarily occurred as more diffuse, shorter-statured cover. Lastly, I expected that the joint analysis of shrub cover change and passerine density would suggest that coarse-scale predictions of future passerine responses to shrub expansion ignore both the highly discontinuous nature of shrub expansion and potential age-class variation in the habitat value of shrub cover.

METHODS

Study Area

The study area is located within the U.S. National Park Service's Arctic and Central Alaska Inventory and Monitoring Networks. I established five long-term monitoring sites targeting passerine assemblages breeding above treeline (Fig. 1). Each site covers an elevational gradient from lowland tundra to alpine habitats, including upland and riparian shrublands, herb- and low shrub–dominated wet tundra, mesic to dry *Dryas* and mixed dwarf shrub tundra, and barren slopes.

Study areas were located at access points, including tundra airstrips in Noatak National Preserve (hereafter, Arctic-west and Arctic-central study areas, respectively), the village of Anaktuvuk Pass within Gates of the Arctic National Park and Preserve (Arctic-east), and along gravel roads in Denali National Park and Preserve (Subarctic-west) and Wrangell-St. Elias National Park and Preserve (Subarctic-east) (Fig. 1). Although study areas covered a variety of topographic settings, they were often centered at valley locations or along passes, which is consistent with the locations of airstrips and scenic roadways. Crews surveyed one study area in each year from 2015 to 2022, except 2021, in which two study areas were surveyed. This effort resulted in resurveys for three of the study areas.

Analyses of Vegetation Cover

I used a timeseries of remotely sensed data representing the proportion of a pixel for which a plant functional type (PFT; e.g., conifers) forms the top of the canopy (hereafter, the PFT data; Macander and Nelson, 2022; Macander et

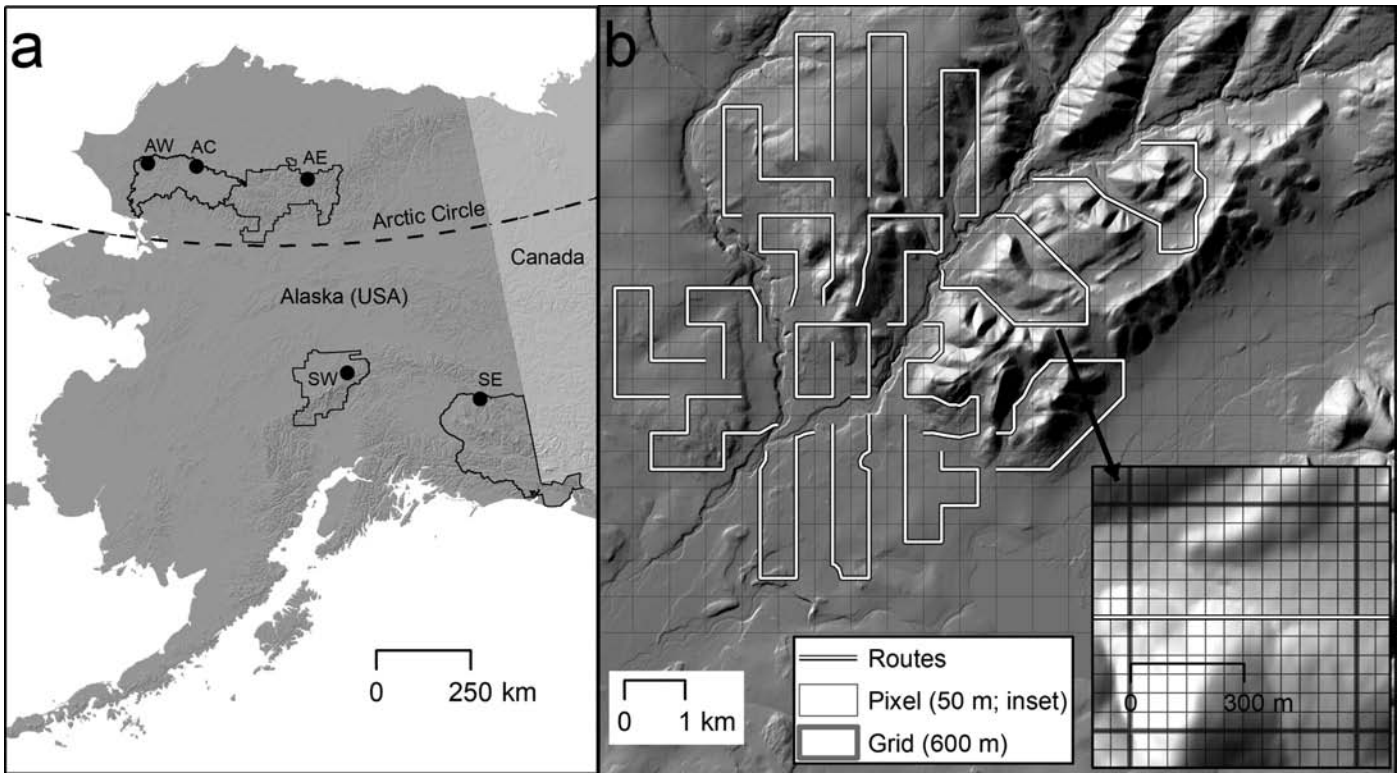

FIG. 1. (a) Location of passerine monitoring study areas in four national parks in Alaska, including: Arctic-west (AW) and Arctic-central (AC) in Noatak National Preserve, Arctic-east (AE) in Gates of the Arctic National Park and Preserve, Subarctic-west (SW) in Denali National Park and Preserve, and Subarctic-east in Wrangell–St. Elias National Park and Preserve (SE). Panel (b) shows an example of the route, plot, and grid configuration. The inset in (b) shows an example 600 m cell overlaid with 50 m pixels and bisected by the survey route.

al., 2022). These values were available for single years at five-year intervals (1985–2020) at a 30 m pixel resolution and are the result of applying a stochastic gradient-boosting approach that integrated spectral, topographic, climatic, permafrost, hydrographic, and phenological covariates (Macander et al., 2022). I used these data to assess topographic correlates of shrub colonization within the five study areas (i.e., the area sampled by the bird survey routes; see *Passerine surveys*). I subsampled these data by systematically selecting 30 m pixels with 60 m spacing, thereby limiting spatial autocorrelation.

At each pixel *i*, I calculated net shrub colonization rates as $z_i = (\%\ cover_{2020,i} - \%\ cover_{1985,i} / (100 - \%\ cover_{1985,i})$ or the rate of transitioning from non-shrub to shrub cover from 1985 to 2020 (Mizel et al., 2023). This transformation accommodated pixel-level variation in the proportion of each pixel that was available for colonization in 1985 and allowed an explicit accounting of a propagule effect (see below). These values were a mixture of zeros and proportions and, consequently, were considered zero-inflated beta random variables with density function:

$$f(z_i|\mu_i,\phi,\alpha_i) = \begin{cases} \alpha_i & \text{if } z_i = 0 \\ (1-\alpha_i)Beta(\mu_i,\phi) & \text{if } z_i \in (0,1) \end{cases}$$

where α_i is the probability of $z_i = 0$ (i.e., the probability of 0 colonization) and μ_i and ϕ are the mean and precision, respectively, of the beta distribution under the parameterization of Ferrari and Cribari-Neto (2004).

I specified logit-linear models for α_i and μ_i using the topographic covariates identified by Mizel et al. (2023), but replaced soil temperature, which was not available for all study areas, with topographic wetness index (TWI) based on previous work documenting a positive relationship between this variable and shrub cover change (Naito and Cairns, 2011). Both models for α_i and μ_i included linear and quadratic terms for elevation, annual solar radiation, TWI, and mean snow-free date (i.e., the Landsat-derived Julian date on which a pixel typically made the transition from snow covered to snow-free; Macander et al., 2015). The model for α_i also included the effect of Gaussian weighted focal shrub cover for 1985, which primarily represented the initial availability of shrub cover (propagules) in the neighborhood of each pixel. The weights were a declining function of distance from the focal pixel, with the scale of the decline being controlled by σ_f under a Gaussian function. The parameter of the Gaussian function was σ_f = 40 m based on the model comparisons of Mizel et al. (2023). TWI was truncated at 12 because larger values in areas of permafrost are often indicative of increasing runoff rather than wetness (e.g., active stream channels; D.K. Swanson, pers. comm. 2023).

I fit these models in a Bayesian framework using the brms package (Bürkner, 2017) as an interface to Stan (Stan Development Team, 2022). I estimated the posterior

distributions of the parameters from four Markov chain Monte Carlo (MCMC) chains, each comprised of 2000 iterations with a 1000 iteration burn-in. I used the default weakly informative priors and assessed convergence visually and using the Gelman-Rubin diagnostic (Brooks and Gelman, 1998). I present predictions as average marginal effects, which represent the combined effects of the covariate on the zero-inflation probability α and the mean of the beta distribution μ with all other covariates held at their means.

Passerine Surveys

I adopted a route-based, continuous-effort survey design to maximize encounter rates of passerines. At the three roadless sites in the Arctic, I centered a grid comprised of 600 m x 600 m cells on the access point (Fig. 1). I used this grid to establish a series of survey routes that radiated outwards from the access point (i.e., the basecamp/airstrip) and covered the accessible portions of the grid within a study area–specific radius ≤ 6.75 km (Fig. 1). At the two Subarctic sites, I centered the grids along gravel roads, which I used as access points for individual survey routes.

I designed the routes to be completed in a single day and to change direction, in part, to return observers close to their original starting point. In general, routes were located such that they intersected the centroid of each cell and then were deflected at an angle of 0 or 90 degrees (i.e., followed a parallel or perpendicular direction; Fig. 1). In some cases, I shifted routes off the central axis of the cell because of to the presence of cliffs and high flow creeks. Each study area contained 12 to 17 routes, which the crew surveyed an average of 2.9 times per season. Routes were fixed after their initial survey, with one exception. In the pilot season (2015), I made adjustments to the routes after their initial visit. However, in subsequent years, the design was refined such that all transects were fixed.

The crew conducted surveys of each route as if they were one continuous line transect, recording one observation per individual bird during a given route visit. Two-person survey teams included a data recorder, who transcribed all encounter information spoken by the observer. Upon detecting a bird, the observer took a bearing and waypoint from their location along the line and used a laser rangefinder to estimate the distance to the bird. I projected encounter locations in continuous space in ArcGIS using the waypoint, bearing, and distance data collected in the field. I only used detections of singing males in analyses.

I delineated plots within each route by buffering the route using a species-specific truncation distance and cutting the buffered area at the intersection of the route and grid cell boundaries (see Fig. 1). Species-specific truncation distances were set to 350–450 m or ~ 3σ where σ is the scale parameter of the detection function (Supplementary Table S1), thereby, minimizing the sensitivity of this parameter to the state-space dimensions (Kéry and Royle, 2016). The purpose of separating the route-level survey strip into multiple plots was primarily to accommodate incomplete route surveys and diurnal variation in song rate. To coincide with peak singing, 90% of surveys were conducted from 03:28 to 09:58 between 24 May and 22 June.

I then overlaid a grid of 50 m pixels on each study area and assigned the encounter locations to the nearest pixel centroid, leading to a data structure that was a series of counts in pixel $i = 1,\ldots I$, in plot $j = 1,\ldots, J$, on visit $k = 1,\ldots, K$, and in year $t = 1$ and 2 (Mizel et al., 2018). For computational expediency in modeling passerine density, the shrub cover data was resampled from its original 30 m resolution to 50 m using bilinear interpolation.

Analyses

Model-based approaches for estimating passerine density typically make inference from the plot-level counts. In doing so, they rely on plot-level effects for explaining spatial variation in density, inducing unexplained variation when density varies within plots due to fine-scale spatial heterogeneity in habitat (Mizel et al., 2018). Point process models describe the organization of individuals in space via the intensity function or the expected density at a given location in space. The point process is described as homogeneous if density is assumed to be constant across space and is termed inhomogeneous in the opposite case. Mizel et al. (2018) developed a Bayesian spatial distance sampling model in which the individual encounters are aggregated at a fine-scale (i.e., a pixel count, as opposed to a plot-level count). Through simulation and applications to Arctic shrub-tundra passerines, they demonstrated that, when density varies within plots, their spatial distance sampling (or pixel count) model had greater capacity for explaining spatial variation in density than models based on the plot-level counts. Shrub expansion is highly discontinuous (e.g., Swanson, 2015), suggesting that a fine-scale assessment of differences in passerine density between long- and recently established shrub cover would be more appropriate and powerful than making this assessment at the plot-level. Thus, I used the pixel count approach of Mizel et al. (2018).

Specifically, I fit spatial distance sampling models (Hedley and Buckland, 2004; Kéry and Royle, 2016; Mizel et al., 2018) individually to each of eight shrub-adapted species with sufficient data for assessing covariates of density at one or more of the study areas (i.e., ≥ 250 singing detections per study area). Species were classified as low shrub–adapted (i.e., American Tree Sparrow [*Spizelloides arborea*], White-crowned Sparrow [*Zonotrichia leucophrys*], Golden-crowned Sparrow [*Zonotrichia atricapilla*], and Savannah Sparrow [*Passerculus sandwichensis*]) and tall shrub–adapted (i.e., Wilson's Warbler [*Cardellina pusilla*], Orange-crowned Warbler [*Leiothlypis celata*], Fox Sparrow [*Passerella iliaca*], and Gray-cheeked Thrush [*Catharus minimus*]) according to the system of Kessel (1979).

TABLE 1. Notation and description of passerine model parameters.

Notation	Description
β_{0g}	Intercept of density specific to study area g
β_{1g}	Study area–specific, linear effect of long-established shrub cover
β_{2g}	Study area–specific, quadratic effect of long-established shrub cover
β_{3g}	Study area–specific, linear effect of recently established shrub cover
β_{4g}	Study area–specific, interaction between long and recently established shrub cover
β_{5g}	Study area–specific, interaction between recently established shrub cover and quadratic, long-established shrub cover
ρ_{0g}	Study area–specific intercept of growth rate
α_{1v}	Date effect on density specific to Arctic (v = 1) and Subarctic (v = 2) study–area groups
α_{2v}	Quadratic date effect on density specific to Arctic and Subarctic study-area groups
α_{3v}	Linear effect of diurnal survey timing specific to Arctic and Subarctic study–area groups
σ_{ε}	Standard deviation of site effects on baseline density
σ_{η}	Standard deviation of site effects on growth rate
σ_{rs}	Scale parameter of the half–normal or hazard–rate detection function specific to observer group r and study–area group s
b_r	Shape parameter of the hazard–rate detection function specific to observer group

These models yielded inference about density of the population that was present (located in the plot) and available for detection (singing). That is, I accommodated imperfect detection via the detection function, which describes the monotonic decrease in detectability with distance from the line. However, the repeated surveys allowed modeling variation in availability (song rate) via a series of nuisance effects (e.g., time of day and Julian date) in a Poisson regression framework (Link and Sauer, 1997; Oedekoven et al., 2013).

Density Model

The focus was on estimating the intensity function for an inhomogeneous Poisson point process of the individual encounter locations (Mizel et al., 2018):

$$\lambda_{ij} = \exp(Z'_{ij}\boldsymbol{\beta}_g + \varepsilon_j)$$

where λ_{ij} is the expected number of individuals per pixel, the $\boldsymbol{\beta}_g$ are the study area–specific vectors of $M \times 1$ coefficients, Z'_{ij} is the corresponding $M \times I \times J$ matrix of spatial covariates, and ε_j are mean zero normal random variables with variance σ^2_{ε} (see Table 1 for model notation). The spatial covariates β_g were specific to each study area g = 1,…G due to previously documented between-study area variation in the scale and topographic setting of shrub expansion (Mizel and Swanson, 2022). They included the linear and quadratic effects of long-established shrub cover ($\%shrub_{1985,i}$), the linear effect of recently established shrub cover ($\%shrub_{2020,i}$–$\%shrub_{1985,i}$), and two interactions (recently established shrub cover with the two long-established shrub cover terms). I included the latter based on the assumption that the effect of one type of cover might depend on the amount of the other type.

Macander et al. (2022) reported large uncertainty around the pixel-level predictions in the PFT data but reliable predictions over larger areas. While I do not accommodate the uncertainty around the PFT predictions in my passerine models, my objective is not to make pixel-level predictions, but rather, to assess the effects of a PFT-derived covariate on passerine density over a large area (the study area). In theory, poor Landsat coverage during the 1980s and 1990s may have resulted in a failure to detect shrub expansion in some sections of my study areas. However, this would have only acted to weaken the effect of the covariate rather than result in spurious conclusions, as Macander et al. (2022) reported low bias for the deciduous shrub predictions (3.6%).

For some species-study area combinations, I lacked sufficient detections for assessing differences in density between long- and recently established shrub cover (Supplementary Table S1). Therefore, I fit reduced models to species–study area combinations with < 250 detections. For study areas with 50–249 detections of a species, I fit a model for density that included linear and quadratic terms for current shrub cover ($\%shrub_{2020}$). For species-study area combinations with < 50 detections, I fit only a study area-specific intercept.

The expected mean plot-level abundance in the baseline year resulted from approximating the integral of the point intensity function via summation over the discretized plot region, $\gamma_{j1} = \Sigma_i \lambda_{ij}$ (Kéry and Royle, 2016). In the instance that a study area was surveyed twice, I assumed a classical exponential growth model for expected mean abundance:

$$\gamma_{j2} = \gamma_{j1} \exp(\rho_{0g} + \varepsilon_j)$$

where ρ_{0g} is the study area–specific mean growth rate and the η_j are mean zero normal random variables for each site with variance σ^2_{η}.

The survey-specific population sizes N_{jkt} were Poisson random variables with expected survey-specific abundance Λ_{jkt}, which accommodated seasonal and diurnal variation around the plot-level abundance γ_{jt}:

$$N_{jkt} \sim Poisson(\Lambda_{jkt})$$

$$\Lambda_{jkt} = \gamma_{jt} \exp(Z'_{jkt}\boldsymbol{\alpha}_v)$$

where Z'_{jkt} is a matrix of observation process covariates, and $\boldsymbol{\alpha}_v$ are vectors of fixed effects coefficients specific for

Arctic and Subarctic study areas, v = 1 and 2, respectively (Table 1). Covariates included the linear and quadratic effects of Julian date and the linear effect of survey timing (Mizel et al., 2021). I calculated the survey timing covariate as time past sunrise for Subarctic study areas and time since 02:00 for Arctic study areas.

Detection Model

I described the observed encounter locations as arising from a spatial point process thinned through incomplete detection. The thinned point intensity μ_{ij} was the product of the expected point intensity and the detection function:

$$\mu_{ij} = \lambda_{ij} \exp\left(-\frac{d_{ij}^2}{2\sigma_{rs}^2}\right)$$

where d is the minimum distance between the route and each pixel and σ_{rs} is the scale parameter of a half-normal detection function for observer group r and study-area group s = {1,2} (Mizel et al., 2018; Mizel and Swanson, 2022). I assigned the study areas to the two classes based on differences in mean shrub cover, which I assumed to affect detectability. The observers were separated into the two classes based upon experience, specifically their total number of surveys from 2015 to 2022. I used a half-normal function for all species except Fox Sparrow and Gray-cheeked Thrush, for which I used the hazard-rate model to fit a shoulder in the function, which was evident under data exploration (Supplementary Table S1). The hazard-rate function has an additional parameter (i.e., the shape parameter) that allows the distance at which detection probability is 1 to extend beyond 0 m (Buckland et al., 2001).

For some species, I lacked sufficient observations for fitting four different scale parameters in the detection function. In such cases, I only fit two different scale parameters, one for each observer group. For the two-parameter hazard rate model, I fit a different shape and scale for each observer group (Table 1).

The model for the observations was decomposed into multinomial and binomial components to avoid specifying the multinomial index as a random variable (Royle et al., 2004; Kéry and Royle, 2016). Conditional on the observed count, the number of individuals observed in a pixel on each plot-visit Y_{ijkt} followed a multinomial distribution with cell probabilities:

$$\pi_{ij} = \frac{\mu_{ij}}{\Sigma_i \mu_{ij}}$$

The observed plot-level counts n_{jkt} were binomial outcomes of the latent population sizes N_{jkt} and the total probability of detection $p_j = \Sigma_i \pi_{ij}$:

$$Y_{ijkt} \left| n_{jkt} \sim multinomial(n_{jkt}, \pi_{ij}) \right.$$

$$\left| n_{jkt} \approx binomial(N_{jkt}, p_j) \right.$$

Assessing the Age Class Effect

I made inferences about differences in passerine density between long- and recently established shrub cover via predictions at specific coverages in the two age classes (e.g., 35% long-established shrub cover and 15% recently established shrub cover). I did this for clarity given that the model included interactions with linear and quadratic terms, and because I expected a limited effect of shrub-cover age at low values of total shrub cover. Further, although the underlying objective was to compare long- and recently established shrub cover, the latter rarely occurs in isolation at the scale of a 50 m pixel. Thus, the predictions were made between stable and expanding shrub cover, where the former was comprised entirely of long-established shrub cover, and the latter was a mixture of long- and recently established shrub cover. In all of these predictive comparisons, total shrub cover (cover present in 2020, including both age classes) was set at 50% due to relatively high density of the target species at this level and the loss of precision at greater values.

I made predictions for stable shrub cover by setting shrub cover established prior to 1985 and shrub cover established between 1985 and 2020 to 50% and 0%, respectively, or {pre-1985 = 50, post 1985 = 0}. I made predictions for expanding shrub cover at study area-specific combinations that maximized sensitivity to differences in age class, either {35, 15} or {40, 10}. The study area–specific choice between these combinations was based on whether the percentage of recently established cover (10% or 15%) was within the 0.83–0.93 quantile for the study area and, consequently, represented a relatively high level of shrub expansion while also yielding reasonable precision in the predicted density.

I fit these species-specific models in a Bayesian framework using JAGS version 4.3.0 (Plummer, 2003) via the runjags package (Denwood, 2016) in program R 4.2 (R Core Development Team, 2022). I specified vague normal priors for all regression coefficients Normal (0, 10), Gamma (0.1, 0.1), priors for the hierarchal precision parameters, and Uniform (0,10) priors for the detection function scale parameters. I estimated the posterior distributions of the parameters from four MCMC chains run for 40,000 iterations and assessed convergence visually and using the Gelman-Rubin diagnostic (Brooks and Gelman, 1998). I scaled continuous covariates (mean = 0, SD = 1) to improve convergence properties.

RESULTS

Correlates of Shrub Colonization

Net shrub colonization rates (1985–2020) peaked broadly at intermediate values of focal shrub cover (1985), suggesting less expansion in pixels that initially had relatively closed canopies and the importance of proximity to pre-existing shrub cover in promoting expansion

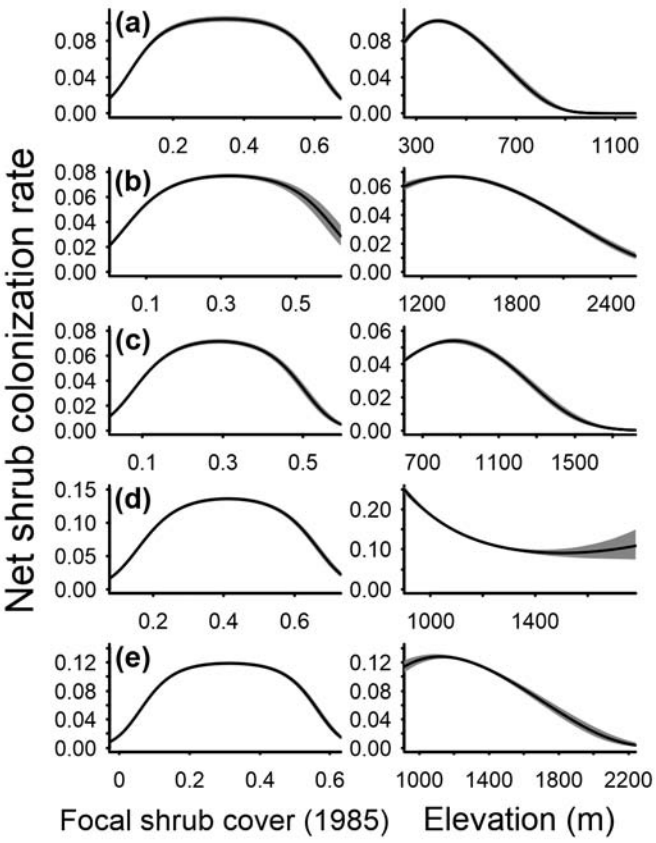

FIG. 2. Average marginal effects of weighted focal shrub cover (1985) and elevation on the net shrub colonization rates for each of the study areas (rows): a) Arctic-west; b) Arctic-central; c) Arctic-east; d) Subarctic-west; and e) Subarctic-east. Colonization rates are the net percentage increase in shrub cover (1985–2020) divided by the percentage of the pixel available to be colonized in 1985 (i.e., initially non-shrub cover). The average marginal effects incorporate the combined effects of the covariate on the zero-inflation probability and the mean of the beta distribution while holding the other covariates at their means. Focal cover in 1985 is based on a Gaussian function with 40 m. The posterior means are shown as solid lines, and the 95% credible intervals have dark grey fill.

(Fig. 2). In addition, colonization rates at all study areas peaked at low elevations (Fig. 2). Colonization rates at Arctic-east showed weak or uncertain effects of mean snow-free date, TWI, and solar radiation (Fig. 3c), likely due to limited shrub expansion overall (Table 2). In contrast, colonization rates at Arctic-west, Arctic-central, and Subarctic-west peaked relatively strongly at intermediate mean snow-free dates (Fig. 3a, b, d). These same three study areas also had colonization rates that peaked at intermediate TWI (Fig. 3a, b, d). Conversely, the colonization rate at

TABLE 2. Percentage of Arctic and Subarctic study areas occupied by shrub cover in 1985 and 2020.

	Percentage of area	
Study area	1985	2020
Arctic-west	17.0	21.0
Arctic-central	14.3	18.4
Arctic-east	11.9	14.8
Subarctic-west	22.2	28.2
Subarctic-east	22.5	28.3

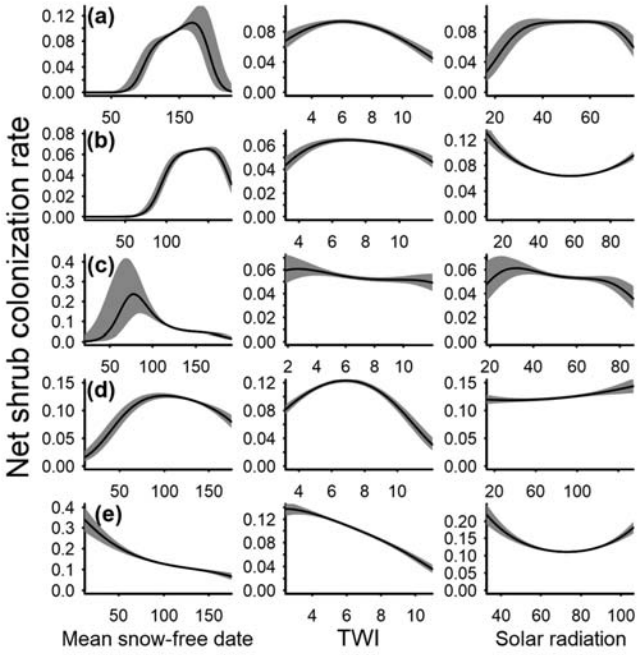

FIG. 3. Average marginal effects of mean snow-free (Julian) date, topographic wetness index (TWI), and annual solar radiation (10,000 Wh/m^2) on the net shrub colonization rates for each of the study areas (rows): a) Arctic-west; b) Arctic-central; c) Arctic-east; d) Subarctic-west; and e) Subarctic-east. Colonization rates are the net percentage increase in cover (1985–2020) divided by the percentage of the pixel available to be colonized in 1985 (i.e., initially non-shrub cover). The average marginal effects incorporate the combined effects of the covariate on the zero-inflation probability and the mean of the beta distribution with the other covariates held at their means. The posterior means are shown as solid lines, and the 95% credible intervals have dark grey fill.

Subarctic-east peaked at early snow-free dates, possibly due to small areas of shrub expansion on wind-scoured sites, and peaked at low values of the TWI, likely due to more pronounced shrub expansion on colluvial slope locations (Fig. 3e). Lastly, a variety of relatively weak responses to annual solar radiation were evident, including bell-shaped (Fig. 3a), u-shaped (Fig. 3b, e), and flat (Fig. 3c, d).

Age Class Variation in Density

All species except Savannah Sparrow, a low shrub–adapted species, had higher point estimates for density in stable shrub cover compared to expanding shrub cover, although 95% credible intervals frequently overlapped between shrub cover types, indicating an overall modest effect of shrub cover age class (Figs. 4, 5). However, the strength of the effect appeared to differ according to habitat association. All low shrub–adapted species showed weak evidence of variation in density between stable and expanding shrub cover (Fig. 4). In contrast, three of 4 tall shrub–adapted species showed some evidence of lower density in expanding shrub cover at Arctic-west (Fig. 5). Specifically, Wilson's Warbler and Orange-crowned Warbler showed considerably lower density in expanding shrub cover, as evidenced by the lack of overlap between 95% credible intervals, while Fox Sparrow showed slightly

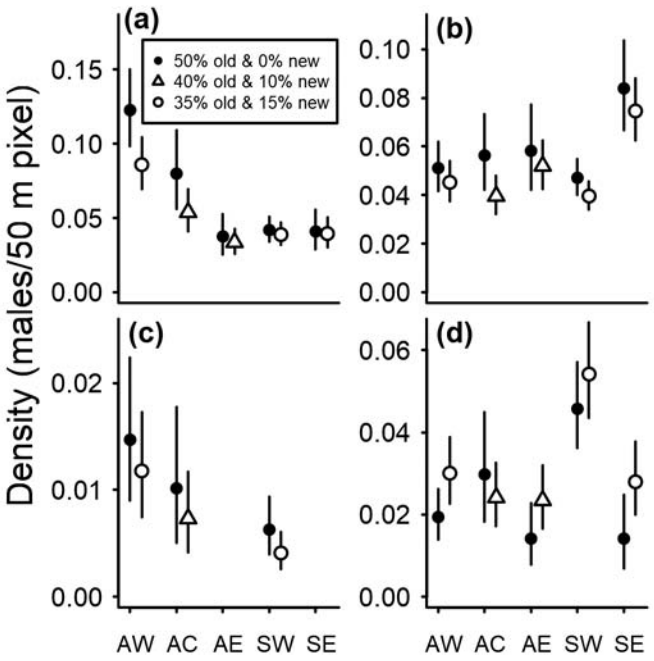

FIG. 4. Posterior means and 95% credible intervals for low shrub–adapted passerine density in stable shrub cover (black points) and expanding shrub cover (unfilled points and triangles) at Arctic-west (AW), Arctic-central (AC), Arctic-east (AE), Subarctic-west (SW), and Subarctic-east (SE) study areas. Estimates are not shown for study area–species combinations where sample sizes did not reach the threshold for estimation. Black points (stable shrub cover) are predictions for 50% shrub cover established prior to 1985 (long-established or old cover) with 0% shrub cover established between 1985 and 2020 (recently established or new cover). Predictions for expanding shrub cover were made at study area–specific combinations of old and new cover that summed to 50%, either 35% old with 15% new (unfilled points) or 40% old with 10% new (unfilled triangles). Species are (a) American Tree Sparrow, (b) White-crowned Sparrow, (c) Golden-crowned Sparrow, and (d) Savannah Sparrow.

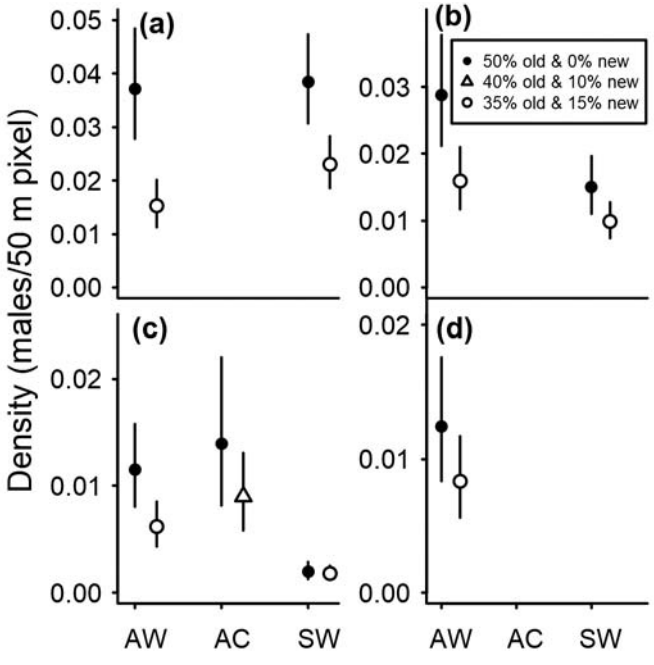

FIG. 5. Posterior means and 95% credible intervals for tall shrub–adapted passerine density in stable shrub cover (black points) and expanding shrub cover (unfilled points and triangles) at Arctic-west (AW), Arctic-central (AC), and Subarctic-west (SW) study areas. Estimates are not shown for study area–species combinations where sample sizes did not reach the threshold for estimation. Black points (stable shrub cover) are predictions for 50% shrub cover established prior to 1985 (long-established or old cover) with 0% shrub cover established between 1985 and 2020 (recently established or new cover). Predictions for expanding shrub cover were made at study area–specific combinations of old and new cover that summed to 50%, either 35% old with 15% new (unfilled points) or 40% old with 10% new (unfilled triangles). Species are (a) Wilson's Warbler, (b) Orange-crowned Warbler, (c) Fox Sparrow, and (d) Gray-cheeked Thrush.

weaker evidence of such a reduction based on a lack of overlap between 92% credible intervals (Fig. 5a-c). In addition, Wilson's Warbler showed lower density in expanding shrub cover at Subarctic-west (Fig. 5a).

DISCUSSION

The widespread expansion of deciduous shrubs in tundra regions has led to predictions of areal increases in the habitat of shrub-adapted passerines. For example, Boelman et al. (2015) predicted a 20%–60% increase in the shrub-dominated habitat of White-crowned Sparrow in the Brooks Range foothills of Arctic Alaska by 2050. However, such predictions are often based on coarse-scale models of vegetation change (e.g., a 4.5 km pixel size; Boelman et al., 2015), which fail to accommodate fine-scale spatial heterogeneity in the extent of shrub expansion. Here, this spatial heterogeneity was evident as pronounced topographic gradients in shrub colonization rates. Furthermore, such studies often ignore the potential lack of equivalency in the habitat value of long- and recently established shrub cover. Here, low shrub–adapted species showed weak differences in density between stable and expanding shrub cover, whereas a subset of tall shrub–adapted species had lower density in expanding shrub cover at Arctic-west and Subarctic-west study areas. The contrasting responses of these two groups suggests that expanding shrub cover may occasionally have structural characteristics, such as shorter height and a more diffuse distribution, that are not preferred by tall shrub–adapted passerines. As such, the observed response is partially a feature of the shrub cover data, in that it does not discriminate based on vegetation height, which is an important characteristic in habitat selection by shrub-adapted passerines (Kessel, 1979; Henden et al., 2013; Thompson et al., 2016). Additional support for the role of shrub height in mediating the response to shrub cover age comes from the Savannah Sparrow results. Savannah Sparrow is associated with the lowest range of shrub heights among the species that were considered (Thompson et al., 2016) and had higher point estimates for density in expanding shrub cover at four of five study areas. Although 95% credible intervals overlapped in all of these cases, the Savannah Sparrow results were the only instances in which the point estimates for density in expanding shrub cover were higher.

The floristic composition of expanding shrub cover may represent another mechanism for the observed differences

in passerine density across shrub age classes under the condition that some shrub species are expanding more rapidly. Although I did not assess variation in passerine density as a function of floristic composition, my field observations are consistent with previous findings of a strong positive association of shrub-adapted passerine abundance and the areal extent of willow shrubs (Sokolov et al., 2012; Henden et al., 2013). In addition, I expect that the densities of shrub-adapted passerines in my study areas are lower in alder-dominated cover (particularly on well-drained soils) and in dwarf birch–dominated cover, with the possible exception of Savannah Sparrow densities in areas of prostrate dwarf birch mixed with graminoids. I also expect that a strong positive relationship exists between the density of shrub-adapted passerines and the coverage of *Salix pulchra,* which is a primary shrub species within water tracks in my study areas.

The relatively sparse occurrence of shrub expansion within the study areas and aspects of my inferential approach limited my capacity for detecting variation in passerine density between stable and expanding shrub cover. Specifically, the depiction of shrub age as discrete (pre- or post-1985) would be expected to yield a weaker response compared to accommodating the fact that shrub establishment occurs over continuous time. Nonetheless, the observed response suggests that the habitat value of areas of expanding shrub cover could vary across species, space, and time. For instance, the observed differences across study areas in the response of tall shrub–adapted passerines likely partially reflect variation in the timing of shrub establishment.

Furthermore, the observed differences in passerine density between stable and expanding shrub cover were documented at a single point in time and could ultimately reflect a lag between the appearance of shrub cover expansion in its initial form and the development of tall, large thickets preferred by tall shrub-adapted passerines. Thus, the observed differences may be relatively transitory, although the duration of this lag could vary spatially.

While variation in passerine density as a function of shrub age and lagged responses to shrub expansion have received little attention for tundra regions, differences in passerine abundance, community composition, and fitness in relation to forest-stand age are well documented. For example, studies from the eastern deciduous forests of the United States show higher abundance of many forest-dependent passerines in stands subject to natural disturbance regimes that are characteristic of old-growth forest and a more diverse canopy structure (Bakermans and Rodewald, 2009; Villard and Jonsson, 2009; Sheehan et al., 2014). Similarly, old-growth shrublands may have structural characteristics, including potentially greater height, denser thickets, and larger canopy volumes, that are preferred by shrub-adapted birds.

I found pronounced topographic gradients in shrub colonization rates, emphasizing the well-documented capacity of portions of tundra landscapes to resist shrub expansion (e.g., Tape et al., 2012; Swanson, 2015). At all study areas, shrub colonization rates depended strongly on proximity to propagules or the initial presence of some adjacent, non-negligible cover. In addition, all study areas had colonization rates that peaked at low elevations, which is consistent with patterns of shrub expansion documented elsewhere in Alaska (Rinas et al., 2017; Brodie et al., 2019). In general, shrub colonization rates peaked at intermediate TWI and snow-free dates, with the latter result indicating that shrub establishment was inhibited on sites that were wind-scoured or had deep, persistent snowpack (Swanson, 2015). Together, these results suggest the importance of assessing vertebrate responses to shrub expansion at spatial scales that are fine enough to accommodate the discontinuous nature of shrub expansion.

The modest nature of differences in passerine density between stable and expanding shrub cover partially reflects the relatively small areal extent of shrub expansion in the study areas within a 35-year period. Unless the rate of expansion accelerates, recently established cover will remain relatively sparse and interspersed with long-established cover, making a difference in passerine density between coarse age classes difficult to detect at any point in time and potentially less important at broader spatial scales. Despite these caveats, the observed differences in passerine density between stable and expanding shrub cover suggest caution in assuming uniform responses to shrub expansion across species and spatial regions. These findings also indicate the potential importance of incorporating time lags into assessments of vertebrate responses to shrub expansion.

ACKNOWLEDGEMENTS

I thank the Nunamiut and Arctic Slope Regional Corporations for access to their lands. I thank the technicians that conducted surveys over the course of this project, particularly Jared Hughey, Sarah Swanson, and Shelli Swanson. We thank Carol McIntyre for help with logistics, and Dave Swanson, Josh Schmidt, Maggie MacCluskie, Eric Wald, and two anonymous reviewers for comments on drafts of this manuscript. No potential conflict of interest was reported by the authors. This study was funded by the US Department of the Interior, National Park Service, Inventory & Monitoring Program in the Central Alaska and Arctic Inventory and Monitoring Networks.

REFERENCES

Bakermans, M.H., and Rodewald, A.D. 2009. Think globally, manage locally: The importance of steady-state forest features for a declining songbird. Forest Ecology and Management 258:224–232. https://doi.org/10.1016/j.foreco.2009.04.010

Boelman, N.T., Gough, L., Wingfield, J., Goetz, S., Asmus, A., Chmura, H.E., Krause, J.S., Perez, J.H., Sweet, S.K., and Guay, K.C. 2015. Greater shrub dominance alters breeding habitat and food resources for migratory songbirds in Alaskan Arctic tundra. Global Change Biology 21(4):1508–1520. https://doi.org/10.1111/gcb.12761

Brodie, J.F., Roland, C.A., Stehn, S.E., and Smirnova, E. 2019. Variability in the expansion of trees and shrubs in boreal Alaska. Ecology 100(5): e02660. https://doi.org/10.1002/ecy.2660

Brooks, S.P., and Gelman, A. 1998. General methods for monitoring convergence of iterative simulations. Journal of Computational and Graphical Statistics 7(4):434–455. https://doi.org/10.1080/10618600.1998.10474787

Buckland, S.T., Anderson, D.R., Burnham, K.P., Laake, J.L., Borchers, D.L., and Thomas, L. 2001. Introduction to distance sampling: Estimating abundance of biological populations. Oxford: Oxford University Press.

Bürkner, P.-C. 2017. brms: An R package for bayesian multilevel models using stan. Journal of Statistical Software 80(1):1–28. https://doi.org/10.18637/jss.v080.i01

Denwood, M. 2016. The runjags package. http://runjags.sourceforge.net.

Ferrari, S., and Cribari-Neto, F. 2004. Beta regression for modelling rates and proportions. Journal of Applied Statistics 31(7):799–815. https://doi.org/10.1080/0266476042000214501

Hedley, S.L, and Buckland, S.T. 2004. Spatial models for line transect sampling. Journal of Agricultural, Biological, and Environmental Statistics 9:181–199. https://doi.org/10.1198/1085711043578

Henden, J.-A., Yoccoz, N.G., Ims, R.A., and Langeland, K. 2013. How spatial variation in areal extent and configuration of labile vegetation states affect the riparian bird community in Arctic tundra. PLoS One 8(5): e63312. https://doi.org/10.1371/journal.pone.0063312

Kéry, M., and Royle, J.A. 2016. Applied hierarchical modeling in ecology: Analysis of distribution, abundance and species richness in R and BUGS, Vol. 1: Prelude and static models. New York: Academic Press. https://doi.org/10.1016/B978-0-12-801378-6.00001-1

Kessel, B. 1979. Avian habitat classification for Alaska. The Murrelet 60(3):86–94. https://doi.org/10.2307/3534270

Link, W.A., and Sauer, J.R. 1997. Estimation of population trajectories from count data. Biometrics 53(2):488–497. https://doi.org/10.2307/2533952

Macander, M.J., and Nelson, P.R. 2022. ABoVE: Modeled top cover by plant functional type over Alaska and Yukon, 1985–2020. ORNL DAAC. https://doi.org/10.3334/ORNLDAAC/2032

Macander, M.J., Swingley, C.S., Joly, K., and Raynolds, M.K. 2015. Landsat–based snow persistence map for northwest Alaska. Remote Sensing of Environment 163:23–31. https://doi.org/10.1016/j.rse.2015.02.028

Macander, M.J., Nelson, P.R., Nawrocki, T.W., Frost, G.V., Orndahl, K.M., Palm, E.C., Wells, A.F., and Goetz, S.J. 2022. Time–series maps reveal widespread change in plant functional type cover across Arctic and boreal Alaska and Yukon. Environmental Research Letters 17(5): 054042. https://doi.org/10.1088/1748-9326/ac6965

McDermott, M.T., Doak, P., Handel, C.M., Breed, G.A., and Mulder, C.P.H. 2021. Willow drives changes in arthropod communities of northwestern Alaska: Ecological implications of shrub expansion. Ecosphere 12(5): e03514. https://doi.org/10.1002/ecs2.3514

Mizel, J.D., and Swanson, D.K. 2022. Hindcasts of passerine density in Arctic and subarctic Alaska suggest noncomplementary responses to shrub expansion by tundra- and shrub-adapted species. Arctic, Antarctic, and Alpine Research 54(1):25–39. https://doi.org/10.1080/15230430.2022.2034373

Mizel, J.D., Schmidt, J.H., and Lindberg, M.S. 2018. Accommodating temporary emigration in spatial distance sampling models. Journal of Applied Ecology 55(3):1456–1464. https://doi.org/10.1111/1365-2664.13053

Mizel, J.D., Schmidt, J.H., and McIntyre, C.L. 2021. Climate and weather have differential effects in a high latitude passerine community. Oecologia 195:355–365. https://doi.org/10.1007/s00442-020-04847-x

Mizel, J.D., Schmidt, J.H., Roland, C.A., and McIntyre, C.L. 2023. Tree and shrub expansion at treeline drive contrasting responses in a subarctic passerine community. Journal of Animal Ecology 92(6):1256–1266. https://doi.org/10.1111/1365-2656.13936

Myers-Smith, I.H., Forbes, B.C., Wilmking, M., Hallinger, M., Lantz, T., Blok, D., Tape, K.D., et al. 2011. Shrub expansion in tundra ecosystems: Dynamics, impacts and research priorities. Environmental Research Letters 6(4): 045509. https://iopscience.iop.org/article/10.1088/1748-9326/6/4/045509

Naito, A.T., and Cairns, D.M. 2011. Relationships between Arctic shrub dynamics and topographically derived hydrologic characteristics. Environmental Research Letters 6(4): 045506. https://doi.org/10.1088/1748-9326/6/4/045506

Oedekoven, C.S., Buckland, S.T., Mackenzie, M.L., Evans, K.O., and Burger L.W., Jr. 2013. Improving distance sampling: Accounting for covariates and non-independency between sampled sites. Journal of Applied Ecology 50(3):786–793. https://doi.org/10.1111/1365-2664.12065

Plummer, M. 2003. JAGS: A program for analysis of bayesian graphical models using Gibbs sampling. https://www.r-project.org/conferences/DSC-2003/Proceedings/Plummer.pdf

R Core Team. 2022. R: A language and environment for statistical computing. R Foundation for Statistical Computing, Vienna, Austria. https://www.bibsonomy.org/bibtex/7469ffee3b07f9167cf47e7555041ee7

Rinas, C.L., Dial, R.J., Sullivan, P.F., Smeltz, T.S., Tobin, S.C., Loso, M., and Geck, J.E. 2017. Thermal segregation drives patterns of alder and willow expansion in a montane ecosystem subject to climate warming. Journal of Ecology 105(4):935–946. https://doi.org/10.1111/1365-2745.12737

Ropars, P., and Boudreau, S. 2012. Shrub expansion at the forest–tundra ecotone: Spatial heterogeneity linked to local topography. Environmental Research Letters 7(1): 015501. https://doi.org/10.1088/1748-9326/7/1/015501

Royle, J.A., Dawson, D.K., and Bates, S. 2004. Modeling abundance effects in distance sampling. Ecology 85(6):1591–1597. https://doi.org/10.1890/03-3127

Sheehan, J., Wood, P.B., Buehler, D.A., Keyser, P.D., Larkin, J.L, Rodewald, A.D., and Wigley, T.B. 2014. Avian response to timber harvesting applied experimentally to manage Cerulean Warbler breeding populations. Forest Ecology and Management 321:5–18. https://doi.org/10.1016/j.foreco.2013.07.037

Sokolov, V., Ehrich, D., Yoccoz, N.G., Sokolov, A., and Lecomte, N. 2012. Bird communities of the Arctic shrub tundra of Yamal: Habitat specialists and generalists. PLoS One 7(12): e0050335. https://doi.org/10.1371/journal.pone.0050335

Stan Development Team. 2022. Stan modeling language user's guide and reference manual, Version 2.17. 0. https://mc-stan.org/docs/reference-manual/index.html

Sturm, M., Racine, C., and Tape, K. 2001. Increasing shrub abundance in the Arctic. Nature 411:546–547. https://doi.org/10.1038/35079180

Sturm, M., Schimel, J., Michaelson, G., Welker, J.M., Oberbauer, S.F., Liston, G.E., Fahnestock, J., and Romanovsky, V.E 2005. Winter biological processes could help convert Arctic tundra to shrubland. Bioscience 55(1):17–26. https://doi.org/10.1641/0006-3568(2005)055[0017:WBPCHC]2.0.CO;2

Swanson, D.K. 2015. Environmental limits of tall shrubs in Alaska's Arctic National Parks. PLoS one 10(19): e0138387. https://doi.org/10.1371/journal.pone.0138387

Tape, K.D., Sturm, M., and Racine, C. 2006. The evidence for shrub expansion in northern Alaska and the pan-Arctic. Global Change Biology 12(4):686–702. https://doi.org/10.1111/j.1365-2486.2006.01128.x

Tape, K.D., Hallinger, M., Welker, J.M., and Ruess, R.W. 2012. Landscape heterogeneity of shrub expansion in Arctic Alaska. Ecosystems 15:711–724. https://doi.org/10.1007/s10021-012-9540-4

Tape, K.D., Christie, K., Carroll, G., and O'Donnell, J.A. 2016a. Novel wildlife in the Arctic: The influence of changing riparian ecosystems and shrub habitat expansion on snowshoe hares. Global Change Biology 22(1):208–219. https://doi.org/10.1111/gcb.13058

Tape, K.D., Gustine, D.D., Ruess, R.W., Adams, L.G., and Clark, J.A. 2016b. Range expansion of moose in Arctic Alaska linked to warming and increased shrub habitat. PLoS one 11(4): e0152636. https://doi.org/10.1371/journal.pone.0152636

Thompson, S.J., Handel, C.M., Richardson, R.M., and McNew, L.B. 2016. When winners become losers: Predicted nonlinear responses of Arctic birds to increasing woody vegetation. PLoS One 11(11): e0164755. https://doi.org/10.1371/journal.pone.0164755

Villard, M.-A., and Jonsson, B.G., 2009. Tolerance of focal species to forest management intensity as a guide in the development of conservation targets. Forest Ecology and Management 258(S14):S142–S145. https://doi.org/10.1016/j.foreco.2009.08.034

Wheeler, H.C., Høye, T.T., and Svenning, J.C. 2018. Wildlife species benefitting from a greener Arctic are most sensitive to shrub cover at leading range edges. Global Change Biology 24(1):212–223. https://doi.org/10.1111/gcb.13837